

Copyright Notice

©2005 IEEE. Personal use of this material is permitted. However, permission to reprint/republish this material for advertising or promotional purposes or for creating new collective works for resale or redistribution to servers or lists, or to reuse any copyrighted component of this work in other works must be obtained from the IEEE.

This material is presented to ensure timely dissemination of scholarly and technical work. Copyright and all rights therein are retained by authors or by other copyright holders. All persons copying this information are expected to adhere to the terms and constraints invoked by each author's copyright. In most cases, these works may not be reposted without the explicit permission of the copyright holder.

Statistical Properties of Fading Processes in WCDMA Systems

Marc C. Necker

Institute of Communication Networks and Computer Engineering,
University of Stuttgart
Pfaffenwaldring 47, D-70569 Stuttgart, Germany
Email: necker@ikr.uni-stuttgart.de

Stephan Saur

Institute of Telecommunications
University of Stuttgart
Pfaffenwaldring 47, D-70569 Stuttgart, Germany
Email: saur@inue.uni-stuttgart.de

Abstract—When simulating Radio Access Networks (RANs) on the network level, the representation of the physical layer is an important issue, since the distribution of erroneous frames on the MAC-layer can have a significant impact on the system performance. This paper focuses on the distribution of frame errors in WCDMA systems. We first study the statistical properties of the frame-error distribution as obtained by physical layer simulation. We then compare the statistical properties to those obtained from statistical channel models for both cases with activated and deactivated closed-loop power control. Finally, an envelope based approach to decide on the successful transmission or the loss of a MAC frame is presented and the applicability of this new approach is verified.

I. INTRODUCTION

The simulation of RANs can be divided into two main parts. *Link level simulations* deal with the actual transmission of bits. Results are usually a Bit Error Ratio (BER) or a Block Error Ratio (BLER). *Network simulations* consider protocol aspects above the physical layer. Since link level simulations are time consuming, it is important to decouple both layers and find an appropriate interface. A common approach is to conduct link level simulations and generate traces of block errors used as an input for network simulations. Other approaches implement statistical channel models including the well known Gilbert-Elliott model as well as other Markovian models (e.g. [1]).

Markovian models have been extended to more accurately reflect the channel's fading characteristics. In [2] and [3] the authors present finite-state models for the Rayleigh fading channel, which are based on the level crossing rate of the wireless channel. In [4] the authors consider a WCDMA system with a frequency-selective fading channel and use N -state Markov chains to capture the correlation among errors.

In this paper we show that a flat-fading channel is well suited to describe the block error process in the frequency-selective fading environment of a WCDMA system. We propose a new model for the block error process that solely relies on the envelope calculation of a flat-fading channel. By avoiding the signal-to-noise/interference level in the model, we can directly use the average BLER to calibrate the model. This is advantageous, since it is more convenient to deal with block error ratios on the network level, rather than signal levels.

This paper is structured as follows: In section II, we will introduce the considered statistical metrics and present some

examples for selected UMTS uplink reference channels with deactivated power control. In section III, we detail the receiver structure. Based on this analysis, we derive a substitute flat-fading model for the block error process in section IV and extend this model to higher rate channels in section V. We subsequently study the impact of power control in section VI and validate the flat-fading model in section VII. Finally, section VIII concludes the paper.

II. STATISTICAL PROPERTIES

For network level simulations, the two most important statistical properties of a frame error pattern are the autocorrelation $R_{\text{ff}}(l)$ and the probability density function (pdf) $p_{\text{iat}}(k)$ of the distribution of the number k of error-free frames in-between two erroneous frames. Let f_i be the sequence of transmitted frames, with $f_i = 0$ denoting the successful reception of the frame at discrete time index i , and $f_i = 1$ denoting a loss, we define:

$$R_{\text{ff}}(l) = \lim_{Z \rightarrow \infty} \frac{1}{2Z+1} \sum_{i=-Z}^Z f_i f_{i-l} \quad (1)$$

with $P_{\text{loss}} = R_{\text{ff}}(0)$, and

$$\forall l \in \mathbb{N} : p_{\text{iat}}(k) = P \{ f_l = 1 \cap f_{l+1} = 0 \cap \dots \cap f_{l+k} = 0 \cap f_{l+k+1} = 1 \} \quad (2)$$

[5] investigates the duration of a block error burst, which essentially corresponds to $p_{\text{iat}}(k)$, for different numbers of users in a cell. Here, we limit ourselves to the single-user case and focus on the comparison of different models. Fig. 1 and Fig. 2 show the autocorrelation function $R_{\text{ff}}(l)$ and the pdf $p_{\text{iat}}(k)$ for the two 3G radio channel test cases 1 and 3 defined in [6] as obtained by link level simulations. In particular, we considered the uplink reference measurement channel specified in [7], section A.2. This reference channel provides an information bit rate of 12.2kBit/s with a data block duration T_F of 20ms (also known as Transmission Time Interval, TTI) and deactivated fast power control. The E_b/N_0 was chosen as 4dB. The terminal speeds in test cases 1 and 3 are $v = 3$ km/h and $v = 120$ km/h, respectively.

For test case 1, $R_{\text{ff}}(l)$ is well above the average value for small values of l . This means that frame errors occur in bursts, which is intuitive due to the slow fading process at a speed of

$v = 3 \text{ km/h}$. $R_{\text{ff}}(l)$ floors out at a value of about 0.12, which in this case indicates no correlation. For test case 3, P_{loss} is much lower, since it is easier to handle fades at higher speeds. We also note that there essentially is no correlation between frame errors, since $R_{\text{ff}}(l)$ is approximately constant for $l \neq 0$. p_{iat} goes well along with these results. Note that for test case 3, p_{iat} follows a negative exponential distribution, since the block error process is memoryless.

III. RECEIVER STRUCTURE

In order to be able to develop a simple substitute model for the fading characteristics in a WCDMA system, we will first investigate the system at the block level. In particular, we will study the structure of the receiver. Commonly, a receiver in a WCDMA system employs a RAKE receiver [8], [9] in order to take advantage of the multipath diversity. Figure 4 shows the block diagram of such a RAKE receiver. It consists of J fingers, the output signals of each are summed up yielding the RAKE receiver's output signal $\tilde{r}(t)$. The input to the RAKE receiver is the received signal $r(t)$, which is delayed by τ_j within each finger. Ideally, τ_j corresponds to the delay of a particular multipath ray. Afterwards, the signal is correlated with the spreading sequence and multiplied with the complex conjugate of the multipath ray's gain factor w_j^* .

Those results in this paper which were obtained by link level simulations were based on a receiver structure with a RAKE receiver having J fingers. The RAKE receiver was assumed to be ideal in the sense that it has *a-priori* knowledge of the delays τ_j of the paths of the respective multipath profile. A real RAKE receiver may suffer from erroneously detected fingers which do not detect the wanted signal portion as well as from the loss of fingers which would detect the wanted signal portion. However, both effects will mainly degrade the SNR of the RAKE output $\tilde{r}(t)$ [10]. Moreover, the impact of these effects on the received signal $\tilde{r}(t)$ is similar to the effect of the self interference due to the non-ideal autocorrelation properties, which is already present in our implemented receiver.

Due to the correlation properties of the spreading sequences, the output of finger j is maximum for those multipath rays having a delay of τ_j , and near zero (depending on

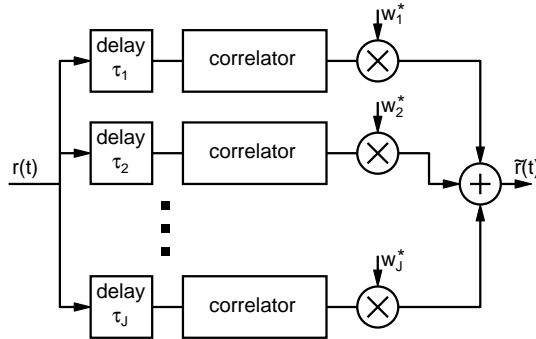


Fig. 4: Block diagram of a RAKE receiver

the sequence's cross-correlation) for all other rays. Consider a typical frequency-selective fading channel according to a wide-sense stationary uncorrelated scattering (WSSUS) model. A widely used model for such a channel was presented by Hoehner in [11]. It describes the channel's time-variant impulse response as

$$h(\tau, t) = \lim_{Z \rightarrow \infty} \frac{1}{\sqrt{Z}} \sum_{m=1}^Z e^{j\theta_m} e^{j2\pi f_{D_m} t} \delta(\tau - \tau_m). \quad (3)$$

The Fourier-Transform of equation (3) with respect to τ yields the channel's time-variant frequency response:

$$H(f, t) = \lim_{Z \rightarrow \infty} \frac{1}{\sqrt{Z}} \sum_{m=1}^Z e^{j\theta_m} e^{j2\pi f_{D_m} t} e^{-j2\pi f \tau_m}. \quad (4)$$

For each of the Z paths, the phase-shift θ_m , the Doppler-shift f_{D_m} and the delay τ_m are randomly chosen from the corresponding probability density function (pdf) $p_\theta(\theta)$, $p_{f_D}(f_D)$ or $p_\tau(\tau)$ of the channel model [11].

In such a model, all multipath rays identified by a particular RAKE finger j sum up to:

$$\bar{h}_j(\tau, t) = \lim_{Z \rightarrow \infty} \frac{1}{\sqrt{Z}} \sum_{m=1}^Z e^{j\theta_m} e^{j2\pi f_{D_m} t} \delta(\tau - \tau_j). \quad (5)$$

where the sum has been normalized to one again. Note that this assumes idealized correlation properties. In reality, all rays which arrive within one chip duration of the delay τ_j will be identified by a particular finger.

It is well known that eq. (5) represents the fading behavior of a frequency non-selective flat-fading channel. As a consequence, the output of each finger corresponds to the transmission of the signal via a flat-fading channel. Finally, we expect the output $\tilde{r}(t)$ of the RAKE receiver to behave like a transmission in a flat-fading environment. In the following sections, we will verify this assumption and develop a simple model based on the envelope of a flat-fading channel, which allows us to model the fading and block error behavior of a WCDMA system by simple means.

IV. FLAT-FADING MODEL FOR WCDMA SYSTEMS

A. Flat-fading model

In this section, we analyse the fading process of a flat-fading channel. A Jakes-distribution was assumed for the Doppler spectrum with a maximum Doppler frequency of $f_{D_{\text{max}}}$. The channel was simulated following the model introduced in [11]:

$$h(t, \tau) = \lim_{Z \rightarrow \infty} \frac{1}{\sqrt{Z}} \sum_{m=1}^Z e^{j\theta_m} e^{j2\pi f_{D_m} t} \delta(\tau) = h(t) \delta(\tau). \quad (6)$$

As described in the previous section, for each of the Z paths, the phase-shift θ_m and the Doppler-shift f_{D_m} are randomly chosen from the corresponding pdf $p_\theta(\theta)$ or $p_{f_D}(f_D)$ of the channel model (see also [9]).

The received envelope of such a flat-fading channel will be denoted with $e(t) = |h(t)|$. Figure 5 shows an example of such an envelope. In this simple environment, we can very well assume that block errors are correlated with the envelope

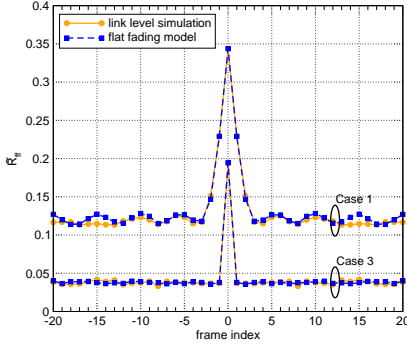


Fig. 1: Autocorrelations $R_{ff}(l)$ for test cases 1 and 3, 12.2kbps UL reference channel

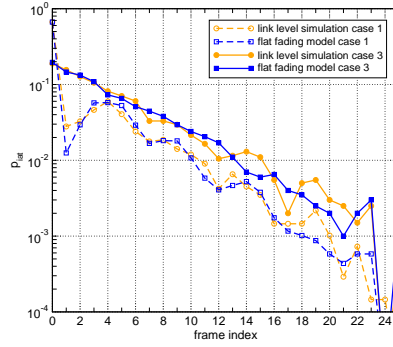


Fig. 2: $p_{iat}(k)$ for test cases 1 and 3, 12.2kbps UL reference channel

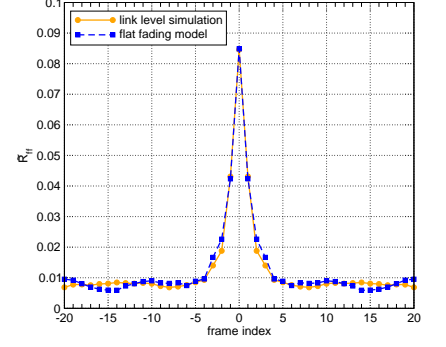


Fig. 3: Autocorrelation functions $R_{ff}(l)$ for test case 1, UL reference channel with 144kBps, $E_b/N_0 = 4$ dB

level $e(t)$. That is, a frame error is more likely to occur if the channel is in a fade. Starting from this, the threshold H_0 is defined such that

$$P\{e(lT_F) \leq H_0\} = P_{\text{loss}}, \quad \forall l \in \mathbb{Z}, \quad (7)$$

where P_{loss} is the target frame error probability. That is, a frame is assumed to be lost whenever the envelope level drops below a certain threshold at the beginning of the frame:

$$f_i = \begin{cases} 0 & \text{if } e(lT_F) > H_0 \\ 1 & \text{if } e(lT_F) \leq H_0 \end{cases}. \quad (8)$$

The threshold H_0 must be chosen based on a target frame error probability. Given a desired P_{loss} , H_0 can easily be chosen such that equation (7) is fulfilled. This is advantageous, since it is often desirable to perform network level simulations with a particular BLER rather than a particular E_b/N_0 .

B. Statistical Properties

Figure 1 shows the $R_{ff}(l)$ for the block error process of this flat-fading model. The parameter H_0 was chosen such that the average block error probability was the same in the WCDMA environment and the flat-fading model. Obviously, the autocorrelations obtained with the flat-fading model are almost identical to the corresponding autocorrelation functions

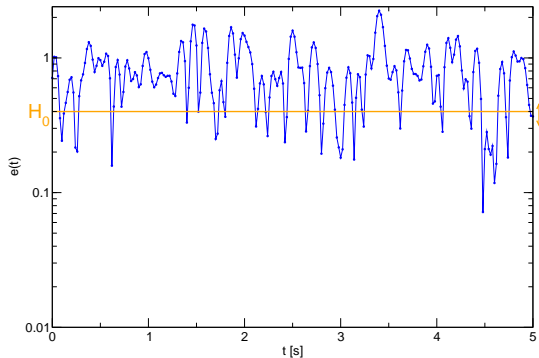


Fig. 5: Example of the envelope of a channel transfer function

of the WCDMA environment. This is an interesting observation, since the physical channels are fundamentally different.

Fig. 2 shows p_{iat} for test cases 1 and 3, respectively. As with the autocorrelation functions, there is a very good match between the flat-fading model and the WCDMA environment. This indicates that the statistical properties of the block error processes in flat-fading environments and in frequency-selective fading environments are very similar due to the RAKE receiver's structure detailed in section III.

V. EXTENSION TO HIGHER RATE CHANNELS

The so far considered 12.2kBps radio bearer transmits only one Radio Block Set (i.e. one data block) within one TTI. This also applies to the higher rate reference channels as defined in [6], annex A.2 and A.3 for uplink and downlink, respectively. This means that the flat-fading model can directly be applied to these higher rate channels.

In contrast to that, [7] annex A.4 specifies uplink reference channels which jointly encode several data blocks. For example, the 144kBps uplink reference channel encodes two data blocks within a TTI of 40ms. Therefore, we need to extend the model in order to be able to decide how many of these data blocks are actually lost. If $f_{i,j}$ corresponds to the j th of the jointly encoded data blocks at time index i , we introduce a second threshold $H_1 < H_0$:

$$f_{i,j} = \begin{cases} 0 & \text{if } e(iT_F) > H_0 \\ \text{rand}(1) & \text{if } H_1 < e(iT_F) \leq H_0 \\ 1 & \text{if } e(iT_F) \leq H_1 \end{cases}, \quad (9)$$

where the result of $\text{rand}(1)$ is 0 or 1 with equal probability.

Fig. 3 shows the autocorrelation functions $R_{ff}(l)$ of the block error process for the UL reference channel with 144kBps and two jointly encoded data blocks within one TTI. Plotted are the autocorrelations obtained by physical layer simulation and by the flat-fading model according to eq. (9). The parameters H_0 and H_1 were chosen such that $R_{ff}(0)$ and $R_{ff}(\pm 1)$ are identical in both cases. Fig. 3 indicates, that the flat-fading model is also suitable for higher rate channels, and can even be applied to channels with jointly encoded data blocks.

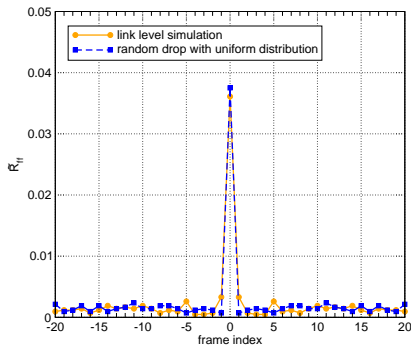


Fig. 6: Autocorrelations $R_{ff}(l)$ for test case 1 with power control, 12.2kbps reference channel, $T_F = 20\text{ms}$

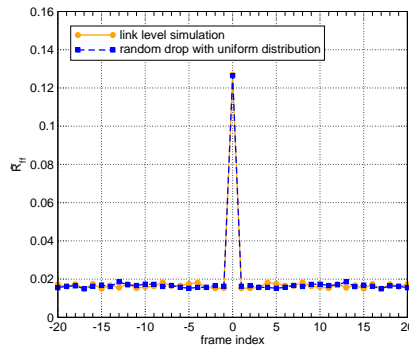


Fig. 7: Autocorrelations $R_{ff}(l)$ for test case 5 with power control, 64kbps channel, $T_F = 10\text{ms}$

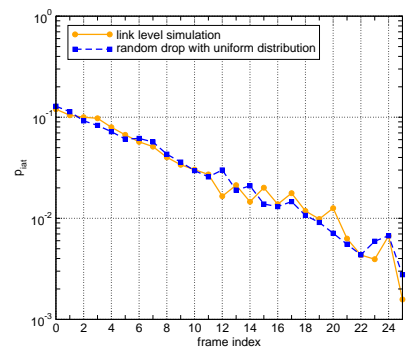


Fig. 8: $p_{iat}(k)$ for test case 5 with power control, 64kbps channel, $T_F = 10\text{ms}$

VI. INFLUENCE OF POWER CONTROL

Figure 6 shows the autocorrelation $R_{ff}(l)$ for the 12.2kbps reference channel with a TTI of $T_F = 20\text{ms}$ with test case 1 and activated power control as it was obtained using link level simulations. The power control was implemented according to the respective UMTS standard. Its purpose is to compensate the fades of the radio channel. Under the assumption of perfect power control, the channel would exhibit no fading. Consequently, block errors would not be correlated. For our physical layer simulations, we assumed non-ideal conditions. Power control commands were received in error with a probability of 0.04 and with a certain delay.

The graph in Fig. 6 unveils that there is almost no correlation between frame losses. Compared to the autocorrelation $R_{ff}(l)$ obtained with a random drop model with uniform drop distribution in Fig. 6, we can observe the expected good match expected from the uncorrelated block errors.

As we go to shorter TTIs, we may expect more correlation in-between block errors, as it is more difficult for the power control to compensate the fast fading effects. Figure 7 plots the autocorrelation $R_{ff}(l)$ for a 64kbps channel with a short TTI of $T_F = 10\text{ms}$ and test case 5 with a mobile speed of 50km/h. Additionally, the graph contains the autocorrelation as obtained with a random drop model. The example shows that even for the short TTI of $T_F = 10\text{ms}$ and at a relatively high speed of 50km/h we can still observe uncorrelated block errors. This fact is also reflected in the good match of the probability density functions $p_{iat}(k)$ for both models in Fig. 8. Again, $p_{iat}(k)$ corresponds to a negative exponential distribution, as it is expected for uncorrelated block errors. We therefore conclude that a random drop model is a very good approximation of the actual system's behavior if closed-loop power control is activated.

VII. VALIDATION OF THE FLAT FADING MODEL

In order to verify the applicability of our flat fading model, we simulated the transmission of IP traffic over the described 144kBit/s DCH with deactivated power control using different drop models for the MAC frames. In all cases we varied the model only in the downlink direction and assumed a random

drop model with a uniform distribution and a BLER of 5% in the uplink direction. Our network level simulations were based on the UMTS simulation model introduced in [12]¹, which models a single cell UMTS system. Note that in this considered single cell environment with a single user, there essentially is no difference between the uplink and the downlink with respect to the IP packet delay at our level of abstraction.

Traffic was generated using a TCP sender with a greedy traffic source. In order to compare the different drop models, we measured the delay of IP packets from the UMTS network's Radio Network Controller (RNC) to the user equipment (UE). From that, we obtained the *IP packet service time* by subtracting the queueing delay of the IP packets in the RNC [12]. In the UE, we measured the interarrival time (IAT) of the IP packets *after* the Automatic Repeat Request (ARQ) and the IP packet reassembly. This includes the effects of in-order delivery of IP packets in the UE.

Figure 9 shows the ccdf of the IP packet service time when using the link level simulation results, the flat fading model and a very simple random drop model with uniform distribution. The model parameters were chosen such that the average drop probability is the same for all models. The results obtained with the flat fading model almost perfectly match the results of the link level simulation. In contrast, the random drop model delivers an essentially different distribution. Additionally, Fig. 10 shows the ccdf of the IAT of the IP packets at the UE for the different drop models. Again, the result obtained with the flat fading model nicely matches that obtained in combination with the link level simulations. As before, the random drop model delivers different statistics. Note, however, that a random drop model is a very good assumption for the case of activated closed-loop power control, as we showed in the previous section.

The distribution of the IP packet service time and IAT is a key factor for the performance of many transport layer protocols and higher layer mechanisms. When doing network simulations, it is therefore essential to model the statistical properties of IP packet transmission as precisely as possible.

¹Note that in contrast to [12], the RLC window size was increased to 2048.

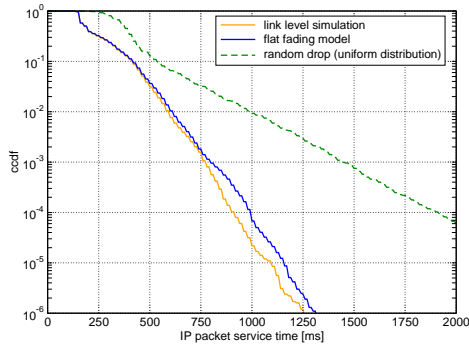


Fig. 9: cdf of the IP packet service time, 144kbps reference channel without power control

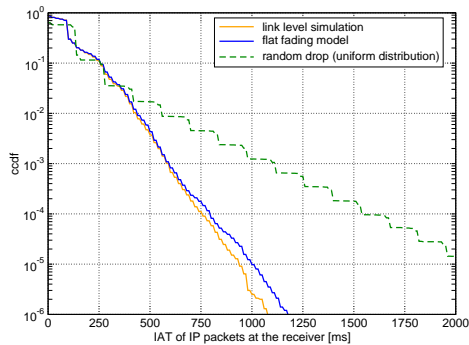


Fig. 10: IAT of IP packets at the receiver side (UE), 144kbps reference channel without power control

VIII. CONCLUSION

An envelope based method to determine the loss of MAC frames in a WCDMA system was presented. The statistical properties of the frame error pattern were evaluated and compared to those of traces obtained from link level simulations and to a random drop model. For the reference cases it was shown that the distribution of frame errors delivered by the envelope based model essentially is the same as that obtained from link level simulations with deactivated power control. The envelope based model was further verified by deploying it in a UMTS network simulator, where the statistical properties on the IP layer essentially matched those obtained if traces

from link level simulations were used. Additionally, we studied the correlation of block errors in the presence of closed-loop power control. We found that even for short TTIs the assumption of uncorrelated block errors is valid, allowing for a convenient modeling of the block error process with a random drop model and a uniform distribution.

ACKNOWLEDGEMENTS

This research work was done in cooperation with Alcatel Research and Innovation Department, Stuttgart.²

REFERENCES

- [1] J. S. Swarts, H. C. Ferreira: "On the evaluation and application of Markov channel models in wireless communications", in *Proc. IEEE VTC 1999-Fall*, pp. 117–121, Amsterdam, September 1999.
- [2] P. Bergamo, D. Maniezzo, A. Giovanardi, G. Mazzini, M. Zorzi: "An improved Markov chain description for fading processes", in *Proc. IEEE ICC 2002*, New York City, New York, Vol. 3, pp. 1347–1351, April 2002
- [3] H. S. Wang and N. Moayeri: "Finite-state Markov channel – a useful model for radio communication channels", *IEEE Transactions on Vehicular Technologies*, Vol. 4, Iss. 1, pp. 163–171, February 1995
- [4] V. Tralli and M. Zorzi: "Markov models for the physical layer block error process in a WCDMA cellular system", in *Proc. IEEE GlobeCom 2002*, Vol. 2, pp. 1925–1929, November 2002
- [5] M. Zorzi, G. Mazzini, V. Tralli, A. Giovanardi: "On the error statistics over a WCDMA air interface", in *Proc. MMT 2000*, Duck Key, Florida, December 2000
- [6] 3GPP TS 25.101: "3rd Generation Partnership Project; Technical Specification Group Radio Access Network; UE Radio Transmission and Reception (FDD)", Release 5, December 2002
- [7] 3GPP TS 25.141: "Base Station (BS) conformance testing (FDD)", Release 6, June 2003
- [8] G. E. Bottomley, T. Ottosson, Y.-P. E. Wang: "A generalized RAKE receiver for interference suppression", *IEEE Journal on Selected Areas in Communications*, Vol. 17, Iss. 8, pp. 1536–1545, August 2000
- [9] G. L. Stüber: "Principles of Mobile Communication", 2nd Edition, 2001, Kluwer Academic Publishers
- [10] T. Pfau: "Two-stage Rake-receiver for UMTS and simulation with several time-variant mobile radio channels", Master Thesis, Institute of Telecommunications, University of Stuttgart, December 2004.
- [11] P. Höher: "A statistical discrete-time model for the WSSUS multipath channel", *IEEE Trans. on Veh. Tech.*, vol 41, pp. 461–468, November 1992
- [12] A. Mutter, M. C. Necker and S. Lück: "IP-Packet Service Time Distributions in UMTS Radio Access Networks", in *Proc. EUNICE 2004*, Tampere, Finland.

²Alcatel SEL AG, Research & Innovation, Lorenzstr. 10, 70435 Stuttgart, Germany. Contact: Andreas Weber (Andreas.Weber@alcatel.de) and Volker Braun (Volker.Braun@alcatel.de).